

10/9-3-92950

Conf-920706--26

SLAC-PUB--5865

DE92 019901

### ACCELERATOR STRUCTURE WORK FOR NLC\*

R. H. Miller, C. Adolphsen, K.L.F. Bane, H. Deruyter, Z. D. Farkas, R. Gluckstern†, H. A. Hoag, N. Holkamp‡, K. Ko, N. Kroll‡, T. Lavine, G. A. Loew, E. M. Nelson, R. B. Palmer, J. M. Paterson, R. D. Ruth, K. A. Thompson, A. Vlieks, J. W. Wang, P. B. Wilson

Stanford Linear Accelerator Center, Stanford, Ca 94309

†University of Maryland.

‡Also Dept. of Physics, UCSD, La Jolla, CA.

§Presently at DESY.

#### ABSTRACT

The NLC design achieves high luminosity with multiple bunches in each RF pulse. Acceleration of a train of bunches without emittance growth requires control of long range dipole wakefields. SLAC is pursuing a structure design which suppresses the effect of wakefields by varying the physical dimensions of successive cells of the disk-loaded travelling wave structure in a manner which spreads the frequencies of the higher mode resonances while retaining the synchronism between the electrons and the accelerating mode. The wakefields of structures incorporating higher mode detuning have been measured at the Accelerator Test Facility at Argonne. Mechanical design and brazing techniques which avoid getting brazing alloy into the interior of the accelerator are being studied. A test facility for high-power testing of these structures is complete and high power testing has begun.

#### GAUSSIAN DETUNING

The cell and iris diameters of the proposed NLC structure vary monotonically with position so that for the most troublesome HOM, the HEM<sub>110</sub> dipole mode, the cell frequencies have a Gaussian density distribution [1,2,3,4]. This produces an integrated wakefield from a bunch as seen by a trailing bunch which has an approximately Gaussian envelope as a function of the time or distance separating the two. The Gaussian density distribution has two advantages over the linear taper of dimensions which gives an approximately uniform frequency distribution. First, the envelope of the integrated wakefield of a uniform distribution has a  $(1/at)\sin(at)$  dependence which decreases much more slowly than the Gaussian. If the design places the bunches at the nodes,  $\sin(at) = 0$ , the beam pulse train structure becomes forever locked to the accelerator structure. Secondly, because the mode frequency separation in a Gaussian distribution is not uniform, the recoherence of the wakefields is suppressed. With a uniform HOM frequency distribution the frequency separation is a constant,  $\partial f$  (within tolerances), and the wakefields recohore after a time  $t = (1/\partial f)$ . In the NLC Gaussian design,  $\sigma_\omega/\omega$  is 2.5% which limits the minimum bunch spacing to about 1.4 ns. The Gaussian distribution is truncated at  $\pm 2\sigma_\omega$ , so the full frequency distribution is 10% wide. This when combined with a variation in disk thickness (discussed below) produces a structure which is over compensated for

attenuation, so that the average accelerating field actually rises by about 20% from the input end to the output end in the absence of beam loading. With full beam loading (90 bunches of  $.65 \times 10^{10}$  particles at 1.4 ns spacing) the field droops by about 20%.

A structure to test Gaussian detuning has been measured at the Accelerator Test Facility at Argonne [5] where a low intensity witness bunch samples the longitudinal and transverse wakefields of a preceding high intensity bunch. These measurements confirm our calculations.

#### END EFFECTS

The NLC structure fundamental mode group velocity varies from 0.11 c at the input to 0.03 c at the output. The lowest dipole mode group velocity actually reverses sign from forward wave at the input to backward wave at the output. Thus dipole fields excited in the beginning of the structure propagate forward into the interior until they hit the 0-mode stop band for their frequency somewhere in the interior. Conversely, dipole fields induced near the output propagate backwards towards the middle. Bane and Gluckstern [6] have calculated the dipole wakefield loss factors, or impedances, for this structure and found that all the modes which are confined to the interior have similar impedances, which are roughly equal to the single cell impedance, but once the modes begin to touch the end of the structure their impedance drops smoothly but rapidly to zero. The result of this is that the distribution of the dipole impedance in frequency which Bane and Gluckstern calculate for the coupled modes is almost identical to the distribution for the uncoupled cells if one uses the synchronous frequency of a periodic structure as the frequency of each cell. In contrast, the lowest dipole band in the SLC (original SLAC) structure is a backward wave throughout the structure, and, as is rather well known, the dipole impedance is dominated by a few modes trapped at the input end of the structure. The worst offender, the lowest frequency mode at 4.14 GHz, has a dipole impedance equal to six cells and causes the beam-break-up observed with long pulses at SLAC [7,8]. What causes the different behavior between the two cases? Simply stated, the conditions for having the mode impedance go smoothly to zero at the ends of a monotonically tapered structure are the following: 1) the beam must be synchronous near the band edge, either near the  $\pi$ -mode or near the

\* Work supported by Department of Energy contract DE-AC03-76SF00515.

Presented at the 15th International Conference on High Energy Accelerator (HEACC '92), Hamburg, Germany, July 20-24, 1992

MASTER

DISTRIBUTION OF THIS DOCUMENT IS UNLIMITED

0-mode; 2) if the synchronous mode is near  $\pi$ , the mode in question must be forward at the low frequency end of the structure and backward at the high frequency end of the structure, and vice versa if the 0-mode is synchronous.

We might conclude that having the dipole impedance rising significantly at one end of the structure would be a very serious condition, but since the high impedance modes are all grouped in one region, it may be possible to damp them all effectively with two HOM couplers, one in each plane. The designer should be sure that the couplers are not at a node of a high impedance mode.

#### SUPPRESSION OF HEM<sub>1n1</sub> MODES

Two of the higher order dipole modes (the HEM<sub>111</sub> and HEM<sub>121</sub> modes) have an appreciable impedance (about one order of magnitude below the HEM<sub>110</sub> mode) and are inadequately detuned by the variation in iris aperture  $2a$  and cavity diameter  $2b$ . The natural way to tune these modes is to vary the cavity length  $g$ , which has relatively little effect on TM<sub>m,n,0</sub> modes. Because we wanted to keep the periodic length  $L$  constant, we chose to vary the disk thickness  $t$ , which varies the cavity length,  $g=L-t$ . We have found that varying  $t$  from 1 mm at the input to 2 mm at the output gives the necessary suppression of these two modes.

#### SIMULATIONS

For pulse trains longer than about 20 ns it is necessary to have a Gaussian distribution with more than the 206 modes which are in the lowest dipole band in a single accelerator structure. To accomplish this we generated Gaussian distributions with  $N \times 206$  cells and then generated  $N$  types of structures, where structure type  $n$  (between 1 and  $N$ ) used every  $N$ th cell starting from  $n$ . Tracking simulations through NLC using 800 or 1600 mode frequencies and impedances of the lowest dipole band in four or eight structures with this interleaved Gaussian detuning show no significant emittance growth due to long range dipole wakefields for  $1 \times 10^{10}$  particles per bunch in a 75 bunch train with a 1.4 ns spacing with no HOM couplers. An accelerating gradient of 50 MeV/m was assumed. The  $N$  structure types were arranged in repeated rising numerical sequence. The machine parameter  $B$  varied as the square root of energy.

#### HIGH POWER STRUCTURE TESTS

A high power test facility has been built to permit testing NLC structures at full power, including acceleration of a low current, short pulse (10 ma for 10 ns) beam for RF diagnostic purposes. The test facility can be powered by one or two developmental X-band klystrons. A Binary Pulse Compression system increases the RF peak power by about a factor of about four. This will later be replaced by a SLED II RF pulse compression system. Two 1.8 meter NLC structures can be accommodated in the test facility (when

they are available), which should produce a 180 MeV electron beam when driven in parallel by a single 50 MW klystron with a 1  $\mu$ sec pulse (one is now available). A 30 cavity uniform X-Band structure has recently exceeded 85 MV/m with a 60 ns RF pulse, after about 80 hours of processing. The dark current pulse had the same length as the RF pulse, was about 2 ma peak at 85 MV/m, and 20  $\mu$ A peak at 50 MV/m (Fig. 1). The dark current was very sensitive to the drive frequency. Raising the frequency 1% above the proper operating frequency would increase the dark current by a factor of about 30. There was a leading edge spike on the dark current pulse which lasted for about one filling time (26 ns) which was two to three times as large as the rest of the pulse. This spike was largest when the RF drive pulse had the fastest risetime (about 9 ns), and disappeared when the risetime was increased to about 20 ns. This is probably explained by the increased high frequency content of a fast rise pulse.

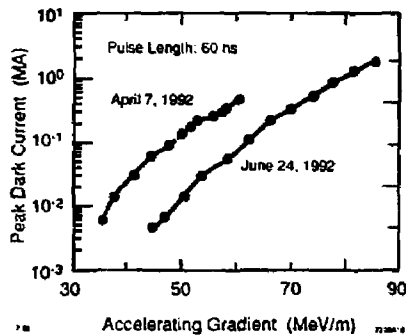


Figure 1. Dark current measurements on 30-cell X-band structure.

#### STRUCTURE FABRICATION STUDIES

We are studying two different structure designs. The first has the passages for the water cooling and vacuum manifolds machined into the individual cell cups before brazing. Pumping calculations indicate that only about one cell in forty needs to have the radial pumping slots shown; the remainder do not have these slots. The second (Fig. 2) has the water cooling passages and vacuum manifolds brazed onto the outside of the RF accelerator brazement.

The advantages of the first approach were seen to be (i) the elimination of multiple brazing steps—the structure is essentially complete after the stack of cells is brazed; (ii) a clean exterior cylindrical surface, coaxial with the beam axis to the best tolerance that state-of-the-art precision machining and cell-to-cell fit-up will allow, and which therefore can be subsequently used as a reference for straightness and alignment checks; (iii) a relatively large ratio of cell diameter to cell thickness, which helps to reduce cell-to-cell axial

misalignment and "book-shelving". However, many disadvantages have become apparent during initial brazing tests. To name a few, (i) the cell is complex and therefore expensive to machine; (ii) large surface areas have to be brazed together—a fact which leads to difficulties in obtaining uniform brazing, due to trapping of by-products of hydrogen reduction and non-uniform surface wetting; (iii) maintenance of cell-to-cell periodic spacing is dependent upon the brazing shim thickness and the amount of diffusion into the copper body of each cell which takes place during the brazing cycle; (iv) leakage paths between adjacent cells are very difficult to locate and may be impossible to fix; (v) many of the possible internal leakage paths in the brazed assembly are between water and vacuum.

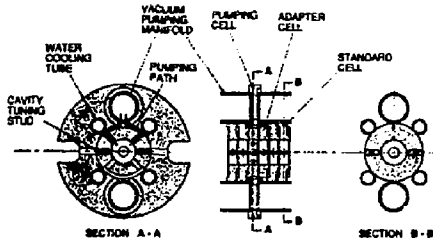


Figure 2. Preferred NLC structure design.

The first test-cells had a knife-edge machined around the rim of each cavity. The idea was that these would make copper-to-copper contact between adjacent cells and exclude braze material from the cavities. However, braze migration does not seem to be a problem when using copper/gold alloys. Detuning due to a small braze fillet is minimal, and two studs built into the walls of each cavity allow for fine tuning during nodal-shift calibration.

The second design approach is expected to be (i) less expensive, because precision (diamond-point) machining is confined to cells which are less complex and about half the diameter, (ii) much easier to leak-check and repair by an extra braze cycle if necessary. The complete 1.8m accelerator section will comprise seven sub-assemblies, each of which can be subjected to mechanical, vacuum and microwave checks before the final assembly braze. The design includes a ventilated annular space between each cell to allow free hydrogen circulation during brazing. Brazing material can be introduced either in the form of shims (which then deteriorates the periodicity tolerance as described above), or as a wire ring, which allows as-machined copper-to-copper fit and very good uniformity of structure periodicity, but gives the possibility of a small virtual leak at each cell interface.

## CONCLUSIONS

Although many confirming calculations and tests remain to be done, equivalent circuit calculations and tracking simulations indicate that frequency detuning of the HOMs is adequate to suppress the effect of long range wakefields for the NLC parameters. High power testing and fabrication studies are underway.

## REFERENCES

1. Deruyter, H., Farkas, Z.D., Hoag, H., Ko, K., Kroll, N.M., Loew, G.A., Miller, R.H., Palmer, R.B., Paterson, J.M., Thompson, K., Wang, J.W., Wilson, P.B., "Damped and Detuned Accelerator Structures", SLAC-PUB-5322, (1990). Presented at 1990 Linear Accel. Conf., Albuquerque, NM, 1990.
2. Thompson, K.A., Wang, J.W., "Simulation of Accelerating Structures with Large Staggered Tuning," SLAC-PUB-5465, (1991). Presented at IEEE Part. Accel. Conf., San Francisco, CA, 1991.
3. Bane, K.L., Holtkamp, N., "A Circuit Model for Obtaining the Coupled Dipole Modes of the NLC Accelerator Structure," SLAC-AAS-63, (1991).
4. Ruth, R.D., "The Development of the Next Linear Collider at SLAC", Proc. of Workshop on Phys. and Experiments with Lin. Colliders, Saariselka, Finland (1991), SLAC-PUB-5729 (1992).
5. Wang, J.W., Loew, G.A., Simpson, J.W., Chojnacki, E., Gai, W., Koneeny, R., Schoessow, P., "Wakefield Measurements of SLAC Linac Structures at the Argonne AATF", Proc. of 1991 IEEE Particle Accel. Conf., Vol. 5, pp. 3219-3221, (1991).
6. Bane, K.L.F., Gluckstern, R.L., "The Transverse Wakefield of a Detuned X-Band Accelerator Structure", SLAC-PUB-5783. Submitted to *Particle Accelerator* (1992).
7. Altenmueller, O.H., Farinholt, E.V., Farkas, Z.D., Herrmannsfeldt, W.B., Hogg, H.A., Koontz, R.F., Kruse, C.J., Loew, G.A., Miller, R.H., "Beam Break-up Experiments at SLAC", Proc. 1966 Linear Accel. Conf., Los Alamos Scientific Lab., LA-3609, 267, (1966).
8. Helm, R., "Computer Study of Wave Propagation, Beam Loading and Beam Blowup in the SLAC Accelerator", Proc. 1966 Linear Accel. Conf., Los Alamos Scientific Lab., LA-3609, 254, (1966).

## **DISCLAIMER**

**This report was prepared as an account of work sponsored by an agency of the United States Government. Neither the United States Government nor any agency thereof, nor any of their employees, makes any warranty, express or implied, or assumes any legal liability or responsibility for the accuracy, completeness, or usefulness of any information, apparatus, product, or process disclosed, or represents that its use would not infringe privately owned rights. Reference herein to any specific commercial product, process, or service by trade name, trademark, manufacturer, or otherwise does not necessarily constitute or imply its endorsement, recommendation, or favoring by the United States Government or any agency thereof. The views and opinions of authors expressed herein do not necessarily state or reflect those of the United States Government or any agency thereof.**